Chapter 2

Experimental techniques: Materials synthesis, Onboard Instrumentation, and Data analyzing tools

2.1 Overview

This chapter covers the experimental methods and characterization techniques used in the thesis. It gives a detailed explanation of sample preparation, fabrication methods, and characterization techniques with their working principles.

This chapter consists of three sections:

1. Material synthesis method technique
2. Characterization techniques which are used for crystal structure analysis, and electrochemical performance analysis of the synthesized materials
3. At last section this chapter covers the kinetics of electrochemical reactions with the help of the Trassati and Dunn methods.

2.2 Synthesis procedure

The synthesis of nanomaterials can be generally categorized under two major approaches: namely, top-down and bottom-up. The former involves methods such as ball milling or sputtering that cause the breakdown of bulk material into nanoscale dimensions, whereas the latter involves creating nanomaterials in an atom-by-atom or molecule-by-molecule manner. Material morphology influences electrochemical properties especially in application to supercapacitor. The choice of the right synthesis method is important in order to produce high-performance electrodes. There are many different techniques that can be employed for the preparation of layered structures based on transition metals, including the sol-gel process,[1] hydrothermal method,[2] microwave irradiation,[3] co-precipitation,[4] chemical-flux method,[5] and solid-state ceramic route.[6] All of them have specific advantages and disadvantages, some of them which are used are listed below.

2.2.1 Sol-gel auto-combustion method

The sol-gel auto-combustion method is a rapid and cost-effective way of synthesizing a wide range of metal oxides and nanoparticles. This method provides a route for the synthesis of nano-sized, homogeneous, and highly mixed elements at an atomic level. A wide range of fuels can be used in the auto-combustion process so that the desired products are synthesized at relatively lower temperatures.[7] Commonly used fuels include citric acid ($C_6H_8O_7$), malic acid $C_4H_6O_5$, dextrose ($C_6H_{12}O_6$), sucrose ($C_{12}H_{22}O_{11}$), urea (CH_4N_2O), and glycine ($C_2H_5NO_2$). Urea, glycine, citric acid and malic acid are strong chelating agents that form complexes with metal cations in solution. These fuels play two important roles: (1) they produce heat by the exothermic reaction through the combustion process, producing CO_2 and H_2O, and (2) they help in the homogeneous mixing of metal cations by forming complexes. Nitrogen, which is not involved in the redox reaction, is released as a gas, thus increasing the porosity of the resultant materials. The type of fuel used mostly determines the strength of combustion reaction.[8]

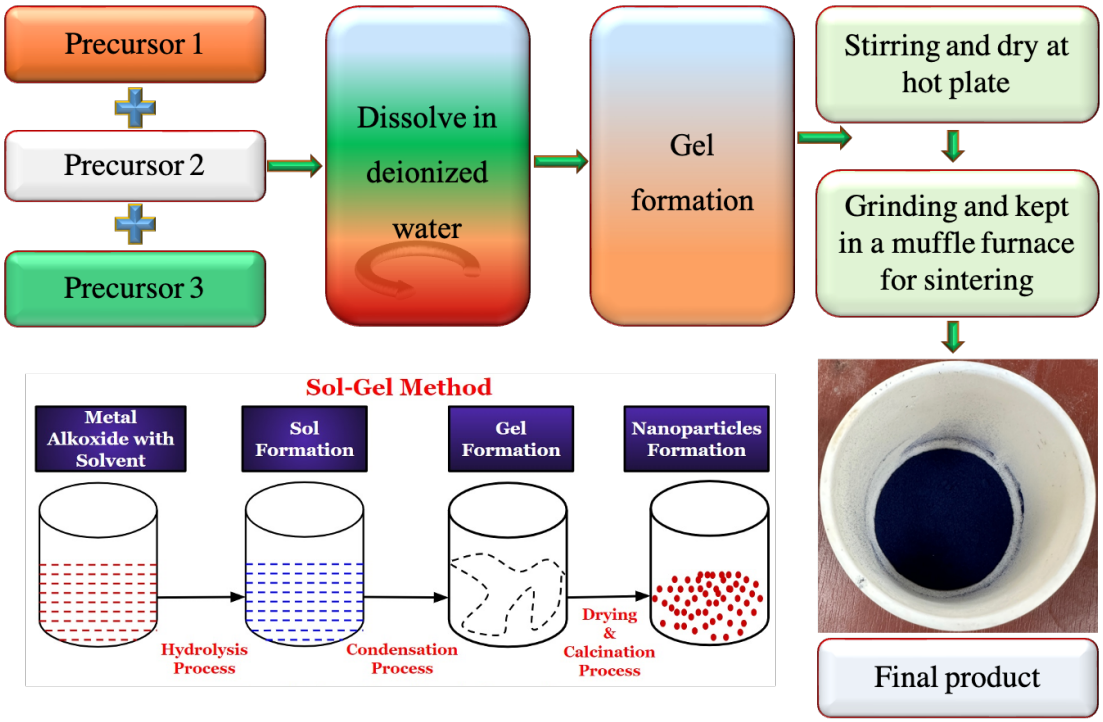

Figure 2.1: Flow chart of synthesis process

2.3 Material Characterization Techniques

This section gives an overview of the characterization techniques used in this study. A summary of each of the techniques is given in the subsequent section. The main techniques used include:

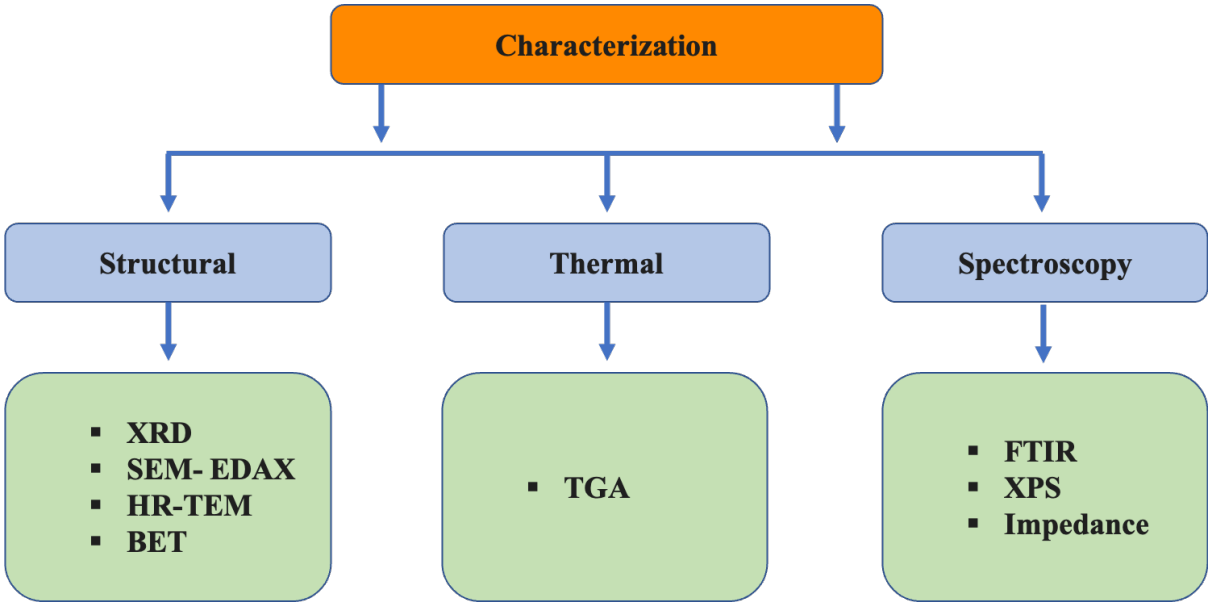

Figure 2.2: Different characterization techniques used for the sample analysis.

2.3.1 Powder X-Ray Diffraction (XRD) analysis

X-ray diffraction, or XRD, is an extremely powerful, noncontact, and non-destructive technique that is suitable for structural analysis. It determines the unique identification of phases within a material and, through the measurement of significant structural properties, determines its phase composition, grain size, preferred orientation, strain state, defect structure, and epitaxy. The data obtained from intensity through XRD provides precise and quantitative information about the atomic arrangement at interfaces. The method, albeit efficient in identifying materials, shows sensitivity to elements in general but is particularly vulnerable to elements with larger atomic numbers due to their large diffracted intensities relative to lighter elements. XRD allows for not only quantitative phase analysis but also qualitative structural and microstructural characterization.

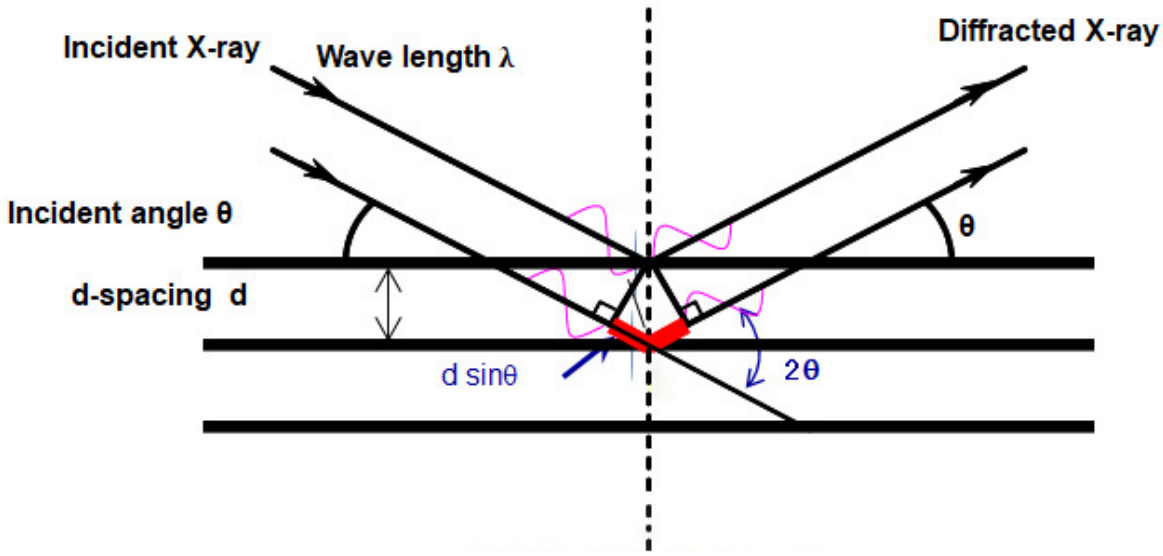

Figure 2.3: Demonstration of Bragg's Law

The diffraction satisfies the Bragg equation:

$$n\lambda = 2dsin\theta \qquad (2.1)$$

Here, d is the spacing between diffracting planes, θ is the incident angle, n is an integer, and λ is the beam's wavelength.[9],[10]

The XRD data were obtained in step-scan mode at a low scanning rate. The phases were characterized by recording the X-ray diffraction pattern at room temperature using an X-ray diffractometer, Rigaku Miniflex 600, Japan with Cu Kα radiation with a wavelength λ = 1.5418 Å at an applied voltage of 40 kV and current of 40 mA. The XRD pattern was recorded from 10° to 90° with a step size of 0.02°. The XRD setup is shown in **figure 2.4**.

Figure 2.4: Rigaku Miniflex 600, XRD Setup, CIFC, IIT (BHU)

2.3.2 Phase Confirmation and Crystal Structure Studies by Powder XRD

X-ray diffraction (XRD) is a versatile, non-destructive technique offering information on the crystallographic structure of natural as well as manufactured materials. Amongst X-rays, the most common used radiation is emitted from copper, with a characteristic wavelength of Cu-Kα radiation (a=1.5418Å). Diffraction takes place in all possible orientation of 2θ when the incident beam strikes a powder sample. The diffracted beam can be detected using a moving detector such as a Geiger counter connected to a chart recorder. In the XRD setup, as in **figure 2.4**, the detector is scanned over a range of values of 2θ at a constant angular velocity. Typically, a range of 2θ from 10° to 80° is enough to pick up most of the significant features of the diffraction pattern. The scanning speed usually is set to about 2θ of 2° per minute, taking about 30 minutes for a complete trace. Extensive structural, physical and chemical information about the substance under study can be withdrawn from X-ray diffraction principles. Various application techniques for various material classes are available that supply specific details of the material studied.

The most significant applications of XRD, be it single-phase or multi-phase material, is the identification of phases. This will help in understanding the mechanism of phase formation and enlighten the relationship between the crystal structure and the properties of the material as put by Neumann's principle.[10]

Hugo Rietveld introduced rietveld refinement in 1960s, which is considered to be one of the broad techniques used for the study of powder X-ray data.[11] The method involves making a fit of a profile calculated with both structural parameters that are instrumental parameters to match or nearly match the experimental data within a non-linear least-square approach. It needs an initial approximation of a number of free parameters, namely, the shape of the peak, dimensions of the unit cell, and atomic coordinates within the crystal structure. Other parameters may be refined iteratively using informed guesses. This procedure allows the detailed refinement of the crystal structure of a powdered material from PXRD data. The success of the Rietveld refinement method relies on three major elements: the quality of the experimental data, the accuracy of the initial model (including approximations), and the user performing the refinement.

A typical diffraction pattern is characterized by the positions, shapes, and intensities of multiple Bragg reflections. Each of these three features provides information: the positions tell about the crystal structure, the shapes tell about sample properties like strain and particle size, and the intensities about both the atomic arrangement in the sample and the instrumentation characteristics.

Table 2.1: Powder diffraction pattern as a function of various crystal structure, specimen, and instrumental parameters[12]

Pattern component	Crystal structure	Specimen property	Instrumental parameter
Peak position	Unit cell parameters (a, b, c, α, β, γ)	• Absorption • Porosity	• Radiation (wavelength), • Instrument/sample alignment • Axial divergence of the beam
Peak intensity	Atomic parameters (x, y, z, B, etc.)	• Preferred orientation • Absorption • Porosity	• Geometry and configuration • Radiation (Lorentz polarization)
Peak shape	• Crystallinity • Disorder • Defects	• Grain size • Strain • Stress	• Radiation (spectral purity) • Geometry • Beam Conditioning

2.3.3 Scanning Electron Microscope (SEM) Analysis

A scanning electron microscope (SEM) uses an electron beam focused to a spot to produce high-resolution images of a sample. Inside the electron gun, in the SEM, there is a cathode that produces both low and high levels of energy electron beams. Such an ability enhances the spatial resolution of the microscope while at the same time minimizing the probability of charging or damage on the sample. The vacuum in the microscope assists in the formation of electrons. The electromagnetic lenses focus the beam to impinge onto the sample, and a variety of electron interaction occurs as a result. A secondary electron detector detects the intensities of these secondary and primary electrons. Then by analysing intensities between them, a sample surface is constructed from an image. Signals of electrons in interacting with sample atoms carry useful information of the morphology of the material and their chemical composition. The image is formed by correlating the position of the beam with the detected signal after the electron beam scans the sample in a raster pattern.[13],[14] The material's image

in this study was obtained using the EVO18 microscope from Zeiss, manufactured in Japan, as shown in **figure 2.5**.

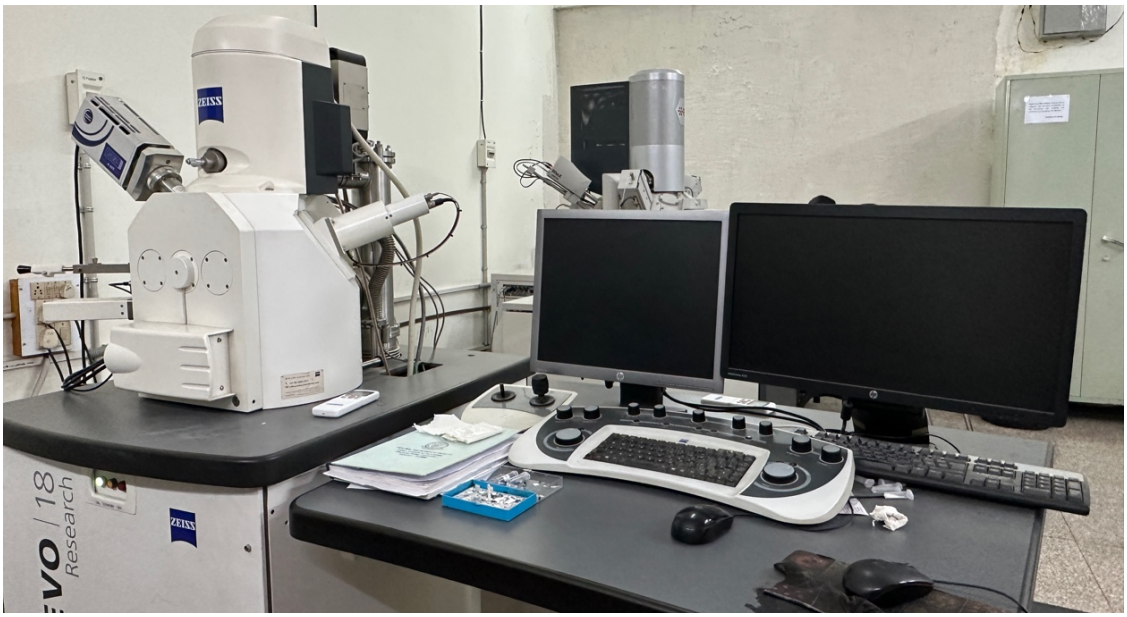

Figure 2.5: SEM Facilities, CIFC, IIT (BHU)

2.3.4 Energy Dispersive X-Ray Spectroscopy (EDAX)

Energy Dispersive X-Ray Analysis, EDX or EDAX is a non-destructive technique used to identify the elemental composition of materials. It is usually integrated with structural analysis tools such as Scanning Electron Microscopy, SEM and Transmission Electron Microscopy, TEM. In this method, a high-energy electron beam interacts with the specimen, ejecting electrons from the inner shell of atomic orbitals. This filling up of inner shell vacancies is done by electrons coming from higher energy levels. These transitions produce characteristic X-rays. The energy of the X-rays emitted allows for determination of the elemental composition of the specimen. However, X-ray mapping might sometimes fail to distinguish elements of interest from unwanted elements if their characteristic X-ray energies are too close, particularly when the energy difference is comparable to the resolution of the spectrometer. Despite such a limitation, the technique offers quantitative analysis by raster scanning the electron beam across the sample, making it ideal for compositional mapping.

This thesis utilized EDAX in conjunction with SEM and TEM for the elemental composition and electron mapping of samples. The **figures 2.5** and **2.7** show SEM and TEM equipment with EDAX spectrometer. [15]

2.3.5 Transmission Electron Microscopy (TEM)

The study of the phenomena at the microscopic level in materials science and engineering has led to the involvement of TEM in this area. A fine powder is prepared, mixed with ethanol, and ultrasonicated for almost 50 minutes in order to ensure a uniform mix and homogenization of the suspension. Then it is drop-cast onto the copper grid and left in the oven at 100 °C overnight. Both diffraction and imaging are used to investigate the samples. TEM is an exceptionally versatile and powerful tool in material characterization, with all available imaging and diffraction modes. BF and DF images are used to study the defects and domain structures; SAD combined with tilting of the crystal helps reconstruct reciprocal space, from which crystal structures and the phase can be identified, in addition to high-resolution lattice imaging for further details on the crystallographic details. In a TEM, there is a transmission of the specimen by a high-energy electron beam (~200 keV). Through their interaction with the sample, the electrons create signals rich in information on the interior structure and chemical composition of the specimen. Electron diffraction patterns and lattice images obtained through TEM provide key crystallographic information required for the detailed analysis of microstructure in materials.

When electrons scatter from a specimen, most of them are elastically scattered by the nuclei of the atoms, and some of them undergo inelastic scattering (as shown in **Figure 2.6**). In comparison with X-ray or neutron diffraction, electron interactions with the specimen are much more extensive and usually include multiple scattering events. In thicker specimens at lower resolutions, such interactions can be treated as an incoherent particle model.

As electrons move near the nuclei, they undergo slight acceleration; as a result, there is a localized reduction in their wavelength, causing a small phase shift. The structural information about the specimen is transferred to the electrons' phase. The elastically scattered electrons are crucial for forming high-resolution images since they retain structural details. In contrast, the inelastically scattered electrons contribute mainly to the image background. However, the inelastic interactions can produce Kikuchi lines in electron diffraction patterns that are valuable for the precise alignment of the specimen in crystallography.[14]

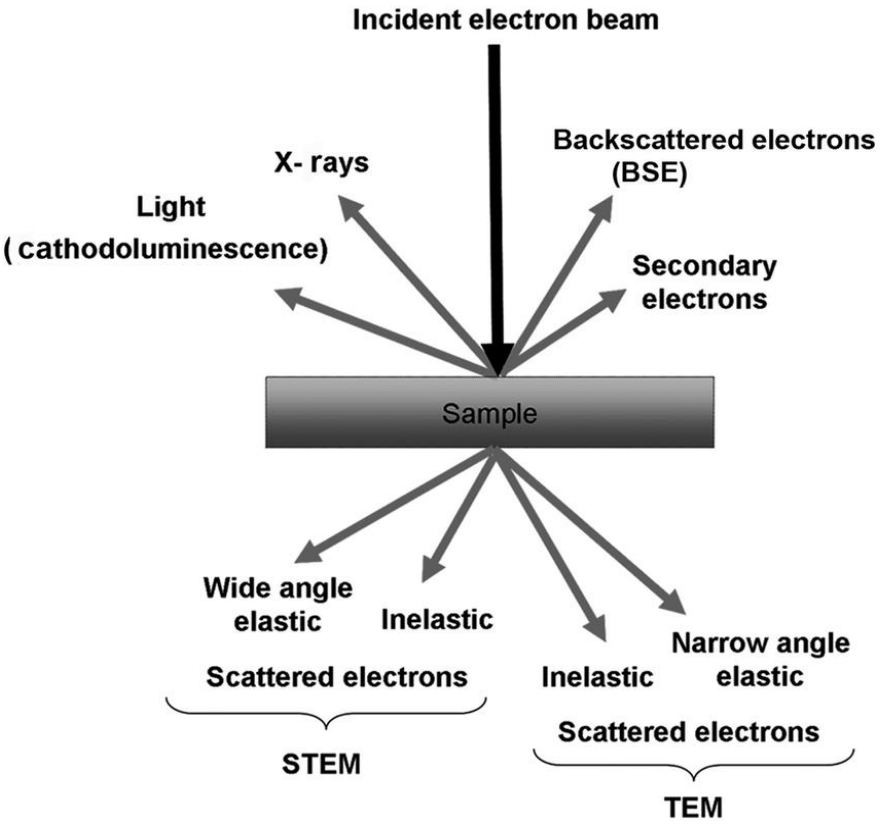

Figure 2.6: Interaction of electrons with sample in TEM analysis [14]

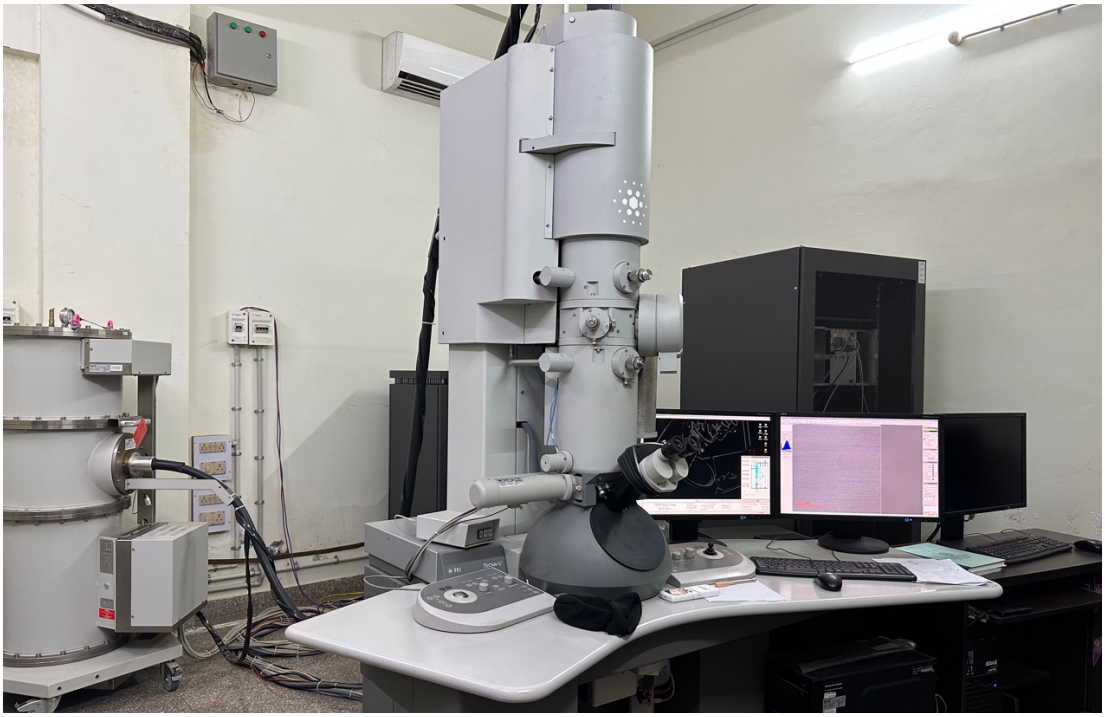

Figure 2.7: TEM facility, CIFC, IIT (BHU)

2.3.6 BET (Brunner-Emmett-Teller theory) Analysis

The BET (Brunauer-Emmett-Teller) method finds applications in the measurement of the specific surface area and the pore size distribution of the material. These surface features determine the properties such as catalytic activity, moisture holding, and shelf life of a material. The BET relies on the physical adsorption of a gas, for instance, nitrogen, onto the solid's surface. This type of adsorption is driven by van der Waals forces between the adsorbate (gas molecules) and the adsorbent (solid surface). Once adsorption occurs, desorption follows, and the amount of gas adsorbed provides a measure of the specific surface area of the sample. The BET process is typically performed at a constant temperature. This is normally done with the help of liquid nitrogen. The process follows isothermal conditions. Gradually, the pressure or concentration of the adsorbate gas is increased. On this, a graph is plotted between the relative pressure of the gas and the volume adsorbed onto the sample.[16],[17]

The BET analysis contains three primary steps:

1. Standardization of the reference cell.

2. Heating the sample to a particular temperature for pre-treatment.

3. Adsorption of the adsorbate on the adsorbent at isothermal conditions.

Figure 2.8: BET (Brunner-Emmett-Teller theory), CIFC. IIT(BHU)

2.3.7 Thermogravimetric analysis (TGA)

TGA, the thermogravimetric analysis is technique that is applied for estimating material's thermal stability. Using this method, it assesses the change of sample mass as a function of temperature which brings out the variation of weight caused by the various procedures like absorption, desorption, phase transitions, and pyrolysis. Within any specified temperature, if mass remains constant with the sample, then such a range determines its being thermally stable. Furthermore, TGA is highly utilized for estimating the calcination temperature. In such calculations, calcination temperature simply refers to that point up to which any degradation in materials starts appearing after going past the range.

Figure 2.9: TGA setup, CIFC, IIT (BHU)

2.3.8 FTIR Spectroscopy

Infrared Spectroscopy, specifically Fourier Transform Infrared (FTIR) Spectroscopy, is a strong analytical technique that will give a "fingerprint" of a sample based on the vibrations of bonds between atoms. Each material produces a different infrared spectrum, due to its unique atomic composition. For this thesis work, the Thermo Scientific Nicolet iS5 FTIR spectrometer was employed, with data collected over the range of 400-4000 cm-1. In the course of FTIR analysis, a beam of light composed of various frequencies interacts with the sample to excite and vibrate the dipole-moisture covalent bonds. Then, there is measurement of the resulting intensity of light by a detector. This interaction eventually creates the interferogram that undergoes the procedure of Fourier transform to know the amount of light at each wavelength absorbed. The characteristic spectrum obtained further helps to identify the various types of bonds present within the material and thus enlighten more on the chemistry composition. FTIR can collect data both in reflected, absorbed or transmitted modes.[19]

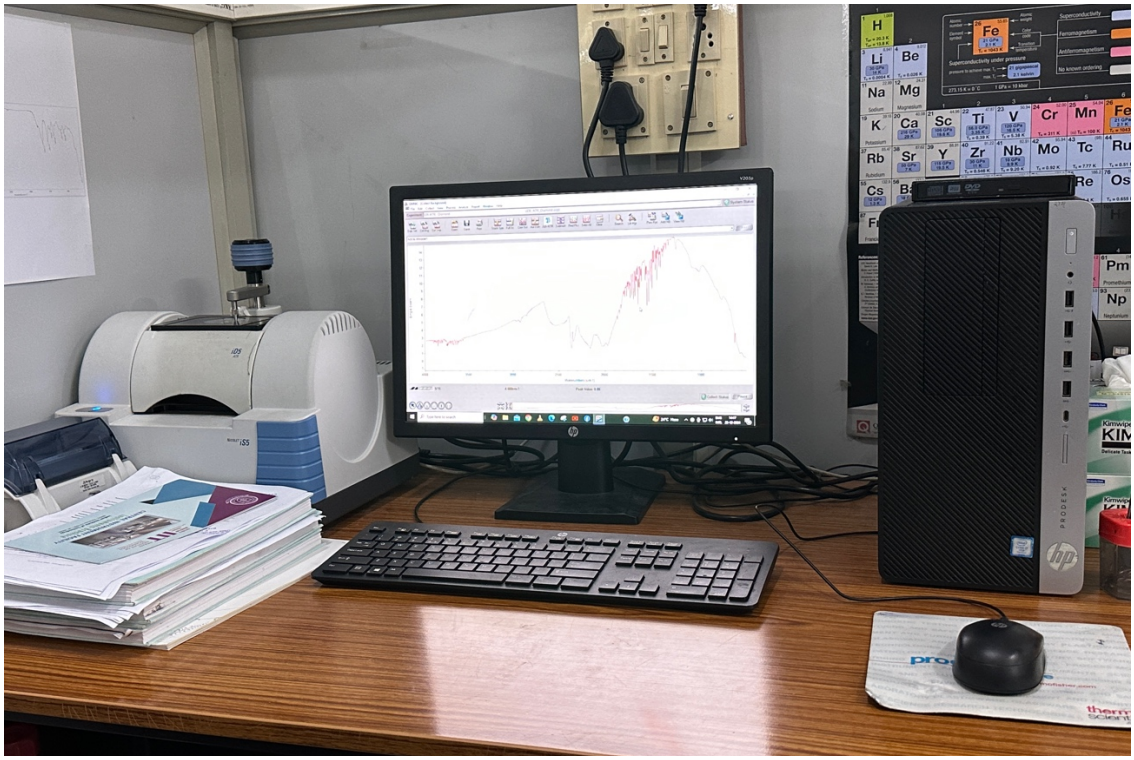

Figure 2.10: FTIR Spectrometer, CIFC. IIT(BHU)

2.3.9 X-ray photoelectron spectroscopy (XPS)

XPS is a technique that is surface-sensitive which is used to analyze composition, electronic states, kinds of bonds, and elements' valence in a given material. In XPS, a sample is exposed to a narrow beam of X-rays, which are then absorbed by the electrons present in the atoms of the sample. This leads to a photoelectron ejection in the sample surface. The energies of these photoelectrons are low, and so their escape depth is on the order of 10 nm, giving information that arises specifically from the surface region of the sample. The energies of the ejected photoelectrons can then be measured and analyzed. By doing this, one determines the atomic species present, as well as the bond types. The energy of the photoelectrons obeys the equation: Ek = hv – EB, where h is the Planck's constant, v is the frequency of the X-ray photon, Ek is the kinetic energy measured by the electron energy analyzer scanning the kinetic energy spectrum and EB represents the electron binding energy of the i-th level. By counting the number of electrons at different binding energies, an energy spectrum is generated, which can

be used to identify the composition and bonding of the sample. It achieves high-resolution HR-XPS if it uses a monochromator for reducing energy dispersion, and hence minimizing the background noise and elimination of unwanted X-rays. Its detection limit for XPS is mostly in the order of parts per thousand while having greater resolution at more extended collection time for signals.[20]

Figure 2.11: X-ray photoelectron spectroscopy (XPS), CIFC. IIT(BHU)

2.3.10 Electrochemical Analysis

2.3.10.1 Electrode Fabrication

Electrochemical measurement was performed to analyze the electrochemical behavior of the pseudocapacitive electrode prepared for the Hybrid Supercapacitor application.

To analyze the electrochemical behavior the working is prepared by adding the active material (in this work that is phosphate-based cathode material), conducting carbon (acetylene black) and binder used as Polyvinylidene Fluoride (PVDF) powders, are weighed with the help of weighing balance to provide the right amount. Then the mixture is well ground in a mortar pestle, after which a small amount of N-methyl pyrrolidinone (NMP) solution is added to

prepare the slurry. For Supercapacitor applications, the slurry is uniformly applied onto Toray carbon paper, which has a coating area of 1 cm^2 with a total mass of around 1 mg, through the use of a micropipette. The synthesized electrodes are immediately placed in an electric oven for drying at 80°C under vacuum overnight. **Figure 2.12** shows the prepared working electrode for the electrochemical study.

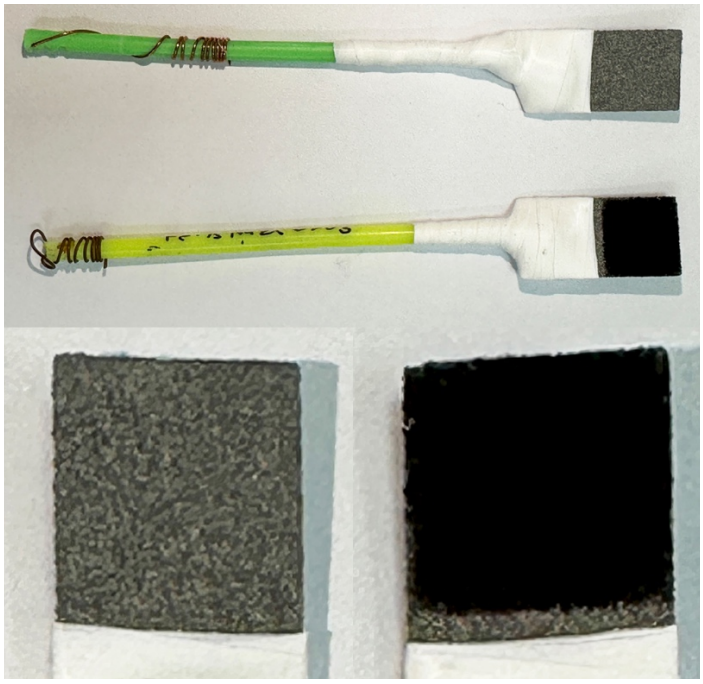

Figure 2.12: Prepared working electrode (coated and non-coated) for the electrochemical testing

2.3.10.2 Three electrode configuration (Half Cell mode)

The three-electrode system includes a working electrode (WE), consisting of active material, and one of the following reference electrodes (RE): Ag/AgCl or a saturated calomel electrode. Lastly, a counter or auxiliary electrode (CE), in platinum wire, completes this set. These are suspended in an appropriate electrolyte solution, aqueous or non-aqueous. It is mainly applied to the investigation of redox properties of active materials and the investigation of chemical processes on the electrode surface with kinetics control either by diffusion or reaction. However, in several cases, some important inconsistencies have been observed while

determining capacitance, energy storage, and power delivery efficiency of devices. Below the diagram illustrates a common three-electrode setup to investigate active material performance:

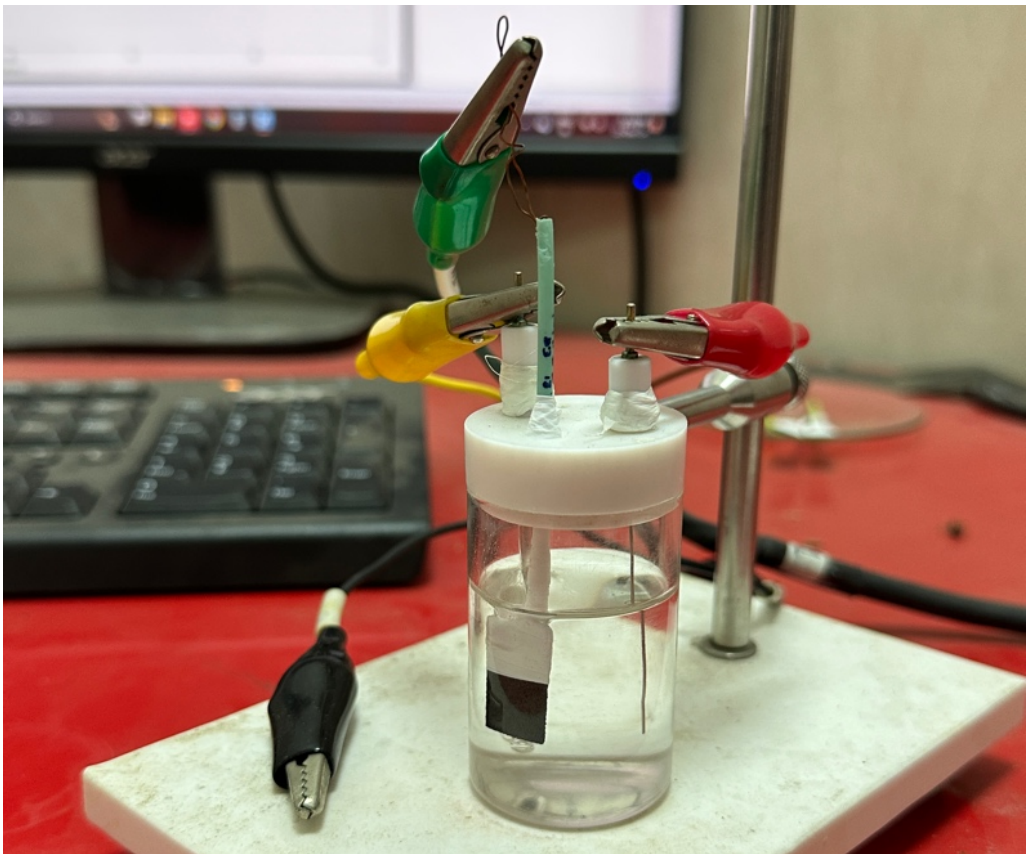

Figure 2.13: Three-electrode arrangement used for the electrochemical measurement

2.3.10.3 Two electrode configuration (Full Cell mode)

In a two-electrode setup, a porous membrane, which has been soaked in an electrolyte, separates two working electrodes. This working electrode is fabricated by covering active materials on a current collector like carbon fiber paper or some metal foils like nickel, gold, or stainless steel. Reference electrodes are usually not found in this arrangement but could sometimes be included to note changes in the potential from charging and discharging processes. This configuration is closely analogous to Supercapacitor or Battery prototypes, making capacitance, energy, and power measurements possible. Commercially available two-

electrode test cells are Swagelok-type cells, coin cells, and pouch cells (**Figure 2.14**),[21] but these may also be fabricated in-house as needed to a specified configuration.

Measurement techniques for two-and three-electrode configurations share the same general approach, though there may be some distinction when one attempts to compare results, carry out calculations, and come up with a comparison, making the proper selection of configuration, especially relevant for specific applications.[22]

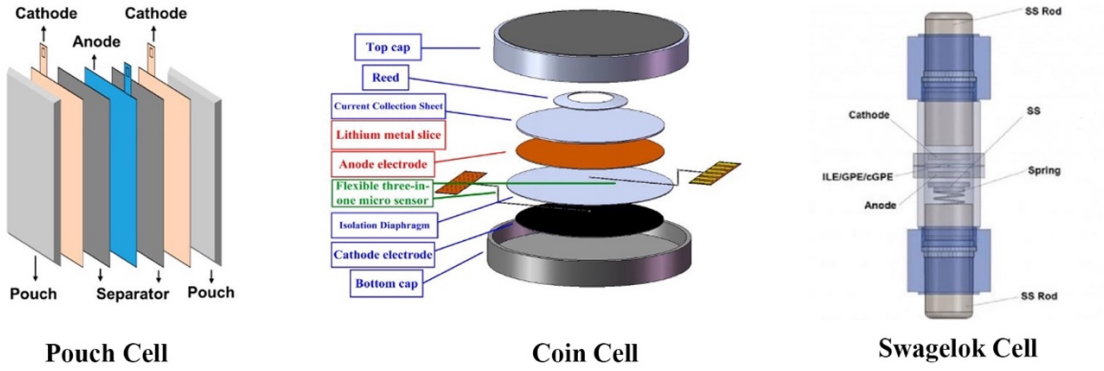

Figure 2.14: Various type of two-electrode configurations[21]

There were three major techniques involved for the measurement of electrochemical performance the electrode material: Cyclic Voltammetry (CV), Galvanostatic charging-discharging (GCD), and Electrochemical Infrared Spectroscopy (EIS).

2.3.10.4 Cyclic voltammetry (CV)

Cyclic voltammetry (CV), is one of the most commonly used techniques in analytical chemistry to study the thermodynamics of redox reactions, the kinetics of electron transfer, and the adsorption behavior of substances on electrodes. Electrochemistry uses cyclic voltammetry to analyze redox reactions, measure specific capacitance, and assess the stability of electrode materials. Voltammograms are graphical plots showing the relationship between applied potential and current density, which are obtained by continuously scanning the potential and measuring the current at the working electrode. A potentiostat creates a potential difference

between the working and reference electrodes and measures the current response between the working and counter electrodes.

The working electrode is the electrode at which the reaction of interest takes place. Typical current collectors for the working electrode include glassy carbon, graphite sheet, and carbon paper, onto which the active material is coated. The counter electrode is an inert electrode, which can be made of platinum, gold, graphite, or glassy carbon that does not participate in the electrochemical reaction. These counter electrodes are used to complete the circuit of current in the electrochemical cell.[23] Reference electrodes, such as Ag/AgCl and the Hg/HgO (saturated calomel electrode (SCE)), are electrodes with well-known electrode potentials.

2.3.10.5 Galvanostatic Charge-Discharge (GCD)

In this method, there is continuous charging and discharging in both three-electrode and two-electrode systems. The potential thus varies with time under a constant applied current. Similar to CV, the curve obtained will include information about the charge storage process, including iR drop, contributions from double-layer and faradic charge storage, and the effective series resistance of the Supercapacitor. However, the results show a difference between three-electrode and two-electrode configurations. When an applied current is passed through, the working electrode has a steep change in its potential due to internal resistance, then gradually changes in accordance with the concentration gradient and over-potential that develop across the surface of the electrode.[24] This GCD technique allows an accurate calculation of the device's specific capacitance, resistance, and cyclic performance. The voltage equation for GCD is given by

$$t = iR + \frac{t}{C}\, i(V) \qquad (2.2)$$

The value of capacitance of the electrode forms the charge- discharge curve can be calculated by:

$$C_{sp} = \frac{i\Delta t}{m\Delta V} \qquad (2.3)$$

2.3.10.6 Electrochemical Impedance Spectroscopy (EIS)

Electrochemical impedance spectroscopy is a technique through which the frequency response of a Supercapacitor can be analyzed by a low-amplitude AC signal, thus ensuring linearity. Through EIS, it is possible to measure the complex impedance and phase angle of the Supercapacitor in a range of frequencies, commonly between 0.01 and 1000 Hz. This leads to two different graphical representations: the Bode plot and the Nyquist plot. While a Bode plot exhibits the relationship of the device with frequency versus the phase angle, on the other hand, Nyquist plots expose not just imaginary impedance values but also those that are real. Then again, the frequency response within EIS is related to that cyclic sweep rate in a voltammogram. The Bode plot is useful in evaluating the gain and phase response of the system; a capacitive behavior is observed with an increasing phase angle up to 90°, while a 45° slope plateau indicates pseudocapacitive response of the electrode material.[25] EIS is also essential for finding the effective series resistance, which aids in accurate calculation of the specific power of a Supercapacitor. The Nyquist plot can be used to analyze the different processes that occur at the electrode surface. The impedance spectrum is usually divided into three segments: a semicircular region in the high-frequency range representing charge transfer resistance, a 45° slope linear portion in the mid-frequency zone, known as the Warburg element, which indicates solid-state diffusion, and a steep slope in the low-frequency region, corresponding to double-layer capacitance.

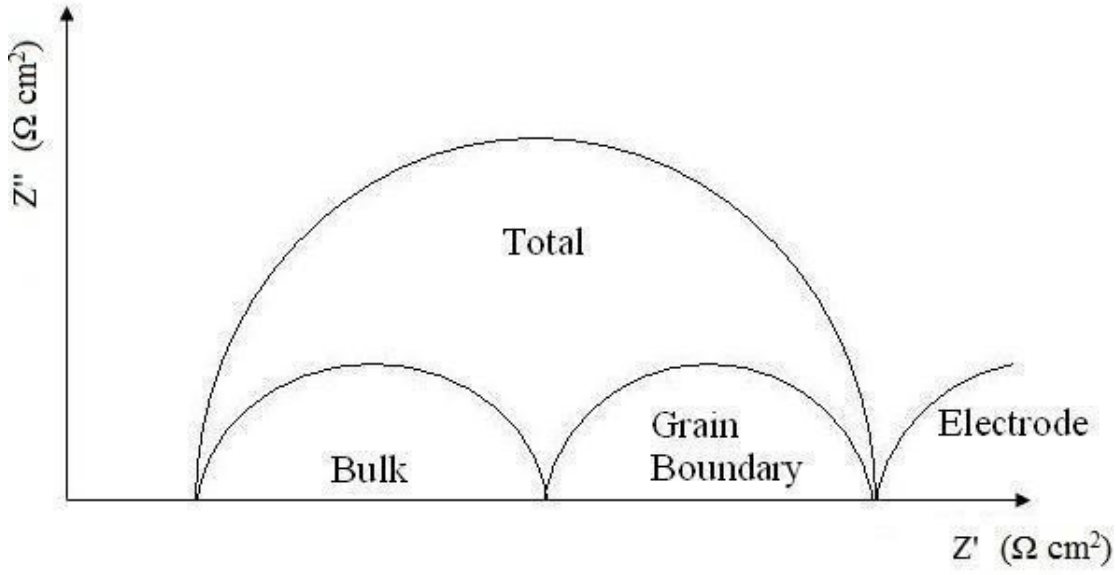

Figure 2.15: Nyquist Plot for ionic solids (Z" = imaginary impedance, Z' = real impedance) [25].

2.3.10.7 Kinetics of the electrochemical reaction by using CV curve

Supercapacitor devices can be classified according to their Current-Voltage response. This section discusses the kinetics of pseudocapacitance in terms of the cyclic voltammetry polarization curve. The electrochemical behavior of pseudocapacitance is described by the following parameters:

1. Linear or pseudo linear relationship between the applied potential and state of charge
2. Nearly ideal electrochemical reversibility
3. Surface-controlled kinetics

Lindstrom et al. performed an experiment on the insertion of Li+ ions into nano porous anatase TiO2 films. They established a simple relationship between the sweep rate and the current observed. Such a relationship is referred to as b-value analysis, which is useful in determining whether the kinetics are surface-controlled/capacitive or semi-infinite diffusion-controlled.[26]

$$\mathrm{i}\,(\mathrm{V}) = \mathrm{a}\, v^{b} \qquad (2.4)$$

$$\log i(V) = \log a + b \log v \qquad (2.5)$$

Where i(V) is the current at a specific potential, ν is the sweep rates, a and b are adjustable parameters, and the b value can be determined as the slope of log(i) vs log(ν) for various sweep rates. When b = 1 is denoted surface control and 0.5 denoted diffusion control. When the b-value falls between 0.5 and 1, the mechanism is attributed to a combination of diffusion and capacitive contributions b value presentation shown in **Figure 2.16**.

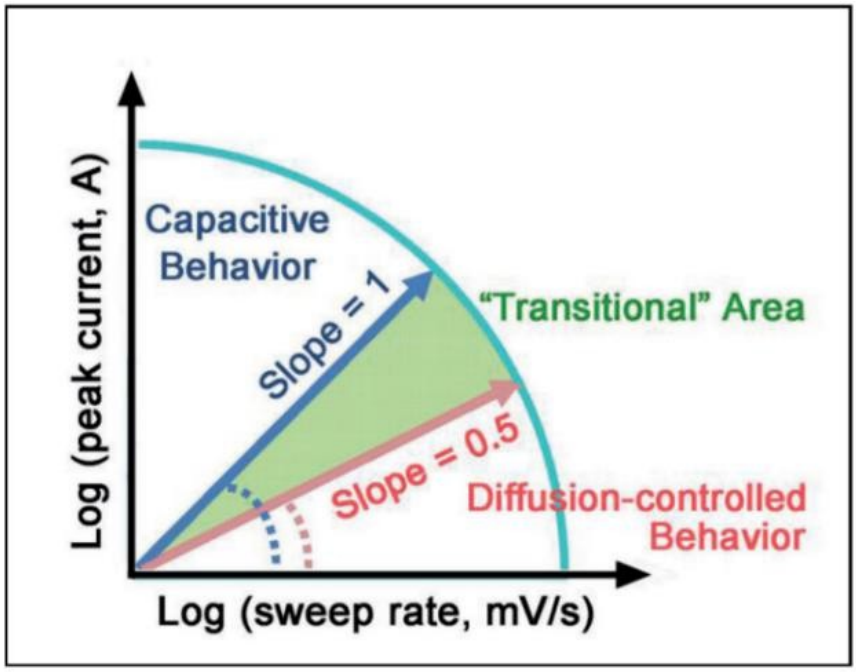

Figure 2.16: Power-law dependence of the peak current on sweep rate for capacitive materials (b= 1.0) and typical battery-type materials (b = 0.5). The "transition" area between capacitive and battery-type materials area is located in the range of b = 0.5–1.0. [26]

Liu et al. proposed a linear combination of surface- and diffusion-controlled currents [27]

$$i(V) = k_1(V)\,\nu + k_2(V)\,\nu^{1/2} \qquad (2.6)$$

Dunn et al. utilized this concept to deconvolute capacitive vs diffusive contributions to the total current for many types of nanostructured transition metal oxides. [28]-[30]

$$i(V)/\nu^{1/2} = k_1(V)\,\nu^{1/2} + k_2\,(V) \qquad (2.7)$$

k_1 and k_2 determine surface and diffusion-controlled processes at specific potentials with multiple sweep rates. The method allows for the separation of the cyclic voltammograms into surface-controlled and diffusion-controlled regions.

Trasatti et al. developed another new method based on voltammetric charge to deconvolute the "inner" (less accessible) and "outer" (more accessible) surface contributions.[31] According to Trasatti, voltammetric charge (Q) can be divided into surface-controlled and diffusion-controlled contributions,

$$Q = Q_s + Q_d \qquad (2.8)$$

Where Q_s and Q_d are the surface-controlled and diffusion-controlled contributions to charge, respectively. Surface-controlled charge contribution also be divided into the "inner" surface contribution, Qs, in, and "outer" surface contribution Q_s, out,

$$Q_s = Q_{s,\,in} + Q_{s,\,out} \qquad (2.9)$$

The "inner" surface contribution is sweep rate dependent (due to lower accessibility of redox sites) and the outer" surface contribution is invariant of sweep rate, assuming semi-infinite linear diffusion and a linear relationship between Q_d and $\nu^{-1/2}$, equation (2.8) can be rearranged to determine Q_s, out when

$$Q = Q_{s,\,out}\, A_1 = + \nu^{-½} \qquad (2.10)$$

Where A_1 is a constant. The y-intercept ($\nu^{-1/2} = 0$; or $\nu = \infty$) determines Q_s. On the other hand, Qs is determined when $\nu = 0$. Assuming Q−1 decreases linearly with $\nu^{1/2}$, equation 2.9 is rewritten as

$$Q^{-1} = Q_s^{-1}\, A_2 \nu^{1/2} \qquad (2.11)$$

Where A_2 is another constant. Q_s^{-1} can be obtained from the y-intercept ($\nu^{1/2} = 0$)

References:

[1] L. Merabet, K. Rida, N. Boukmouche, Ceram Int 2018, 44, 11265.

[2] G. Yang, S.J. Park, Electrochim Acta 2018, 285, 405.

[3] C. Lamiel, V.H. Nguyen, C. Roh, C. Kang, J.J. Shim, Electrochim Acta 2016, 210,

240.

[4] W. Mi, C. Dai, S. Zhou, J. Yang, Q. Li, Q. Xu, Mater Lett 2018, 227, 66.

[5] Y. Ben Smida, R. Marzouki, S. Kaya, S. Erkan, M. Faouzi Zid, A. Hichem Hamzaoui, Synthesis Methods and Crystallization 2020.

[6] S.R. Nalluri, R. Nagarjuna, D. Patra, R. Ganesan, G. Balaji, Sci Rep 2019, 9.

[7] Kessler, V. G., Seisenbaeva, G. A., Unell, M. & Hakansson, S. Chemically Triggered Biodelivery Using Metal-Organic Sol-Gel Synthesis. Angew. Chem. Int. Ed. 47, 8506–8509 (2008)

[8] Dumitrescu, P. Samoila, V. Nica, F. Doroftei, A. Iordan, M. Palamaru Study of the chelating/fuel agents influence on NiFe2O4 samples with potential catalytic properties Powder Technol., 2013, 243, 9-17

[9] Borie, B. X-Ray Diffraction in Crystals, Imperfect Crystals, and Amorphous Bodies. Journal of the American Chemical Society. 1965, pp 140–141.

[10] B. D Cullity, Elements of X- Ray Diffraction

[11] Rietveld, H. M. (2 June 1969). "A profile refinement method for nuclear and magnetic structures". Journal of Applied Crystallography. 2 (2): 65–71.

[12] Pecharsky, V. K., & Zavalij, P. Y. (2009). Fundamentals of Powder Diffraction and Structural Characterization of Materials

[13] Amelinckx, S.; van Dyck, D.; van Landuyt, J.; van Tendeloo, G. Handbook of Microscopy: Applications in Materials Science , Solid-State Physics and Chemistry; 2008.

[14] David B. Williams and C. Barry Carter Transmission electron microscopy, (Plenum, 1996)

[15] EDAX: https://en.wikipedia.org/wiki/Energy-dispersive_X-ray_spectroscopy

[16] Sing, K. S. Adsorption methods for the characterization of porous materials.

Advances in Colloid and Interface Science, 1998, 76, 3-11.

[17] Donohue, M. D.; Aranovich, G. L., Classification of Gibbs Adsorption Isotherms. Adv. Colloid Interface Sci. 1998, 76, 137-152

[18] M.E.Brown , Introduction to thermal analysis : Techniques and application , second edition, Springer, 2007.

19] B. Stuart, Spectral analysis. Infrared spectroscopy: fundamentals and applications, (2004).45-70.

[20] P. Van der Heide, X-ray photoelectron spectroscopy: an introduction to principles and practices. John Wiley & Sons

[21] V. Khomenko, E. Frackowiak, F. Béguin, Electrochim Acta 2005, 50, 2499.

[22] D.A.C. Brownson, C.E. Banks, The Handbook of Graphene Electrochemistry, Springer London2014.

[23] N. Elgrishi, K.J. Rountree, B.D. McCarthy, E.S. Rountree, T.T. Eisenhart, J.L. Dempsey, J Chem Educ 2018, 95, 197.

[24] A.J. Bard, L.R. Faulkner, Electrochemical Methods: Fundamentals and Applications 2001, 156.

[25] D.P. Dubal, S. Abdel-Azeim, N.R. Chodankar, Y.K. Han, IScience 2019, 16, 50.

[26] T. -C. Liu, W.G. Pell, B.E. Conway, S.L. Roberson, J Electrochem Soc 1998, 145, 1882.

[27] Brezesinski, T.; Wang, J.; Polleux, J.; Dunn, B.; Tolbert, S. H. Templated Nanocrystal-Based Porous TiO2 Films for next-Generation Electrochemical Capacitors. J. Am. Chem. Soc. 2009, 131, 1802−1809

[28] Brezesinski, T.; Wang, J.; Senter, R.; Brezesinski, K.; Dunn, B.; Tolbert, S. H. On the

Correlation between Mechanical Flexibility, Nanoscale Structure, and Charge Storage in Periodic Mesoporous CeO2 Thin Films. ACS Nano 2010, 4, 967−977.

[29] Brezesinski, K.; Wang, J.; Haetge, J.; Reitz, C.; Steinmueller, S. O.; Tolbert, S. H.; Smarsly, B. M.; Dunn, B.; Brezesinski, T. Pseudocapacitive Contributions to Charge Storage in Highly Ordered Mesoporous Group v Transition Metal Oxides with Iso-Oriented Layered Nanocrystalline Domains. J. Am. Chem. Soc. 2010, 132, 6982−6990.

[30] Ardizzone, S.; Fregonara, G.; Trasatti, S. Inner" and "Outer" Active Surface of RuO2 Electrodes. Electrochim. Acta 1990, 35, 263−267

[31] Zheng, J. P.; Cygan, P. J.; Jow, T. R. Hydrous Ruthenium Oxide as an Electrode Material for Electrochemical Capacitors. J. Electrochem. Soc. 1995, 142, 2699−2703